Turkish Journal of Physics

http://journals.tubitak.gov.tr/physics/

Research Article

Turk J Phys
(2017) 41: 498 – 506

doi:10.3906/fiz-1704-30

Monte Carlo simulation of a medical linear accelerator for filtered and FFF systems

Çağrı YAZĞAN[1,*], **Yiğit ÇEÇEN**[2]
[1]Department of Nuclear Medicine, Isparta City Hospital, Isparta, Turkey
[2]Department of Radiation Oncology, School of Medicine, Akdeniz University, Antalya, Turkey

Received: 21.05.2017 • **Accepted/Published Online:** 27.07.2017 • **Final Version:** 18.12.2017

Abstract: In order to simulate radiation transport, various algorithms, codes, and programs have been developed. In this study Monte Carlo N-particle code is used to simulate a medical electron linear accelerator gantry for research purposes. Detailed geometry of the LINAC head and water phantom are modeled and simulated for calculations. Analyses are made for filtered and flattening filter-free (FFF) systems. Percent depth dose and dose profile measurements are calculated with Monte Carlo simulations and compared with experimental and theoretical values for quality assurance of the model. Flux, dose, and spectrum analyses are performed for filtered and FFF systems separately. In this study, it was aimed to run the linear accelerator in a computer environment for different purposes, and this aim was achieved.

Key words: Monte Carlo method, Monte Carlo N-particle code, linear accelerator, simulation flattening filter-free

1. Introduction

The Monte Carlo (MC) method is a method that can be used to solve mathematical and physical problems by using simulation techniques. This method allows each photon or particle to be tracked separately under the known physical laws. It is, in principle, the only method capable of computing the dose distribution accurately for all situations encountered in radiation therapy [1]. At present, MC simulation is the most sophisticated and accurate algorithm [2].

MC N-particle (MCNP) code is a general purpose MC code developed by the Los Alamos National Laboratory. With MCNP6, 37 different radiation types can be used for criticality, shielding, dosimetry, detector, and many other applications [3].

In this study, the medical linear accelerator was modeled for the MCNP by using the SuperMC code [4]. It was developed by the FDS team (INES, Chinese Academy of Sciences) and was used for modeling Monte Carlo-based codes.

The linear accelerator works on the principle that under an electric field (alternating), the particle is accelerated during the positive half cycle and retarded during the negative half cycle [5]. Electrons reaching the desired kinetic energy emerge as an electron beam from the device for electron therapy. Figure 1 shows the operating system of the linear accelerator. When photon therapy is applied, high-energy electrons hit a target and bremsstrahlung X-rays are produced. The produced photons preferably emerge from the system either filtered or nonfiltered. The removal of the flattening filter leads to a radially decreasing fluence distribution and thus to inhomogeneous dose distribution [6]. This system is called flattening filter-free (FFF). In order

*Correspondence: cagri.yazgan@gmail.com

to equalize the dose distribution in the horizontal axes of irradiation field, the photon beam is filtered with a flattening filter.

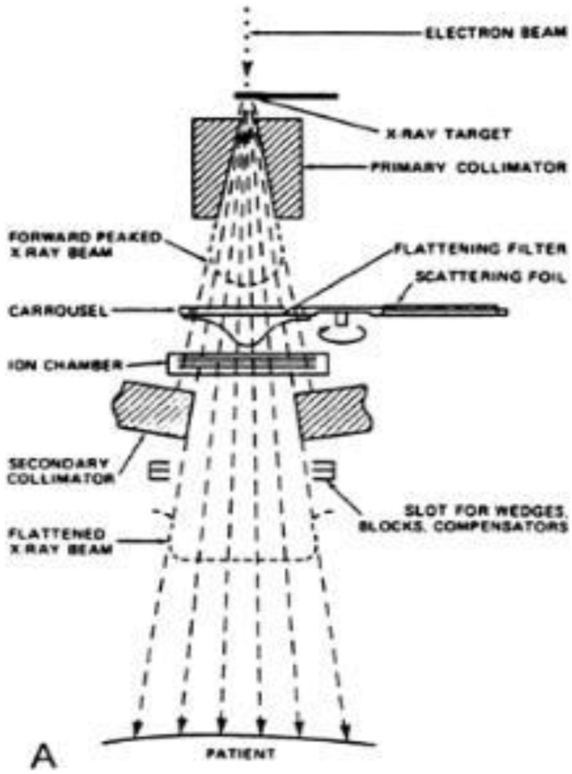

Figure 1. Components of treatment head, X-ray therapy mode [7].

Quality controls were done by comparing the simulated results with the experimental and theoretical results. For this purpose, percent depth dose (PDD) and dose profile measurements were examined as two main measurements to be applied in quality control for filtered and FFF systems in 18-MV photon energy. PDD is a measurement that gives a unique value for a certain set of parameters like beam energy, depth, source skin distance (SSD), and field size [8]. Photons have a characteristic dose maximum depth and dose distribution depending on their energy with depth in water. In the filtered system, an equal dose should be obtained at each point in the irradiation field and this control is provided in the dose profile measurements. After ensuring the quality control of the device, other calculations were investigated.

In addition to medical purposes, linear accelerators have a wide range of uses in nuclear sciences. Linear accelerator models and simulations can also be used for research, development, design, and shielding purposes. The model may be used for the development of a linear accelerator in future studies. The device can be operated at any energy level other than the specific energy levels allowed by medical linear accelerator software.

2. Materials and methods

The first step in the study is the modeling of the linear accelerator head. In order to simulate the machine with actual conditions, position, material content, and dimensions of the components are obtained and measured. The modeled linear accelerator head is shown in Figure 2.

A cylindrical tube with a diameter of 1 cm and a length of 5 cm, in which electrons are directed to the target, is modeled as vacuumed so that electrons do not interact and do not cause any ionization. The target is

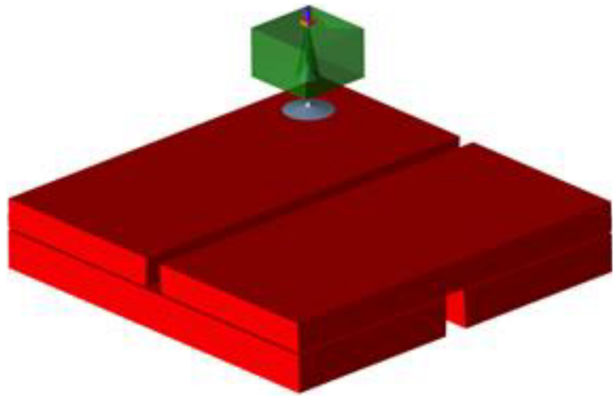

Figure 2. Medical linear accelerator gantry head model.

made of tungsten [9]. Accelerated electrons are bombarded to the tungsten target to produce bremsstrahlung X-rays. A copper holder below the target is modeled to intersect with the vacuum tube so that there is no space between the parts. The copper component holds the tungsten target, filters the X-ray beam, and transfers the heat that is generated as a result of X-ray production. At the end of the copper component, a tungsten primary collimator was modeled. The primary collimator gives a conical distribution to the photon beam. For this reason, there is a conical cavity defined as air inside the primary collimator. When the conical air gap is modeled, the base radius of the cone is calculated considering the irradiation area that can be obtained at a distance of 100 cm from the source. Since the maximum irradiation area to be examined is 40×40 cm^2, the air gap in the primary collimator is calculated with reference to this area. Steel flattening filters are modeled at the air space in the primary collimator and below the primary collimator for use in different energies to achieve a uniform dose profile [9]. The flattening filter is optimized until a proper dose profile is achieved. For the calculations of the FFF system, filters were identified as air and removed from the system. Secondary collimators are components that form the irradiation field to the photon beam. Divergence of the secondary collimator was calculated by the Thales theorem in order to provide the desired field at the surface of the water phantom, which is shown in Figure 3, located at a distance of 100 cm from the target.

The electron source was defined to the code with the source definition card. The source was modeled in a vacuum tube, 1 cm above the tungsten target, to form an electron beam 3 mm in diameter [10]. The beam was directed downward in the vertical axis with a Gaussian distribution of 0.1 MeV at FWHM [11].

The number of particles, flux, and dose measurements of any radiation kind on the cells and surfaces can be obtained by the corresponding tally card. The code was run separately for filtered and FFF systems. In the water phantom for depth-dependent and horizontal calculations, cells with a volume of $0.25 \times 1 \times 1$ cm^3 were modeled. For the photons, dose, flux, and spectrum were investigated. The F4 (particle/cm^2) tally was used for the flux and spectrum, while the *F8 (MeV) tally was used for the dose calculations. For spectrum analysis, tally scores were grouped separately depending on their energy. Photons generated at the energy range of 0 to 18 MeV were recorded in 1789 channels of 10-keV energy intervals and this tally was worked as a multichannel analyzer. The simulation was run for 10^9 source electrons.

The results of the MCNP code are uncertain because the simulation is run with a certain number of source particles. Uncertainty has to be reduced by variance reduction techniques as much as possible with various methods [12]. The main method used to shorten the calculation time and reduce the uncertainty is the use of an importance card. The importance card is identified on the cell card to determine which radiation

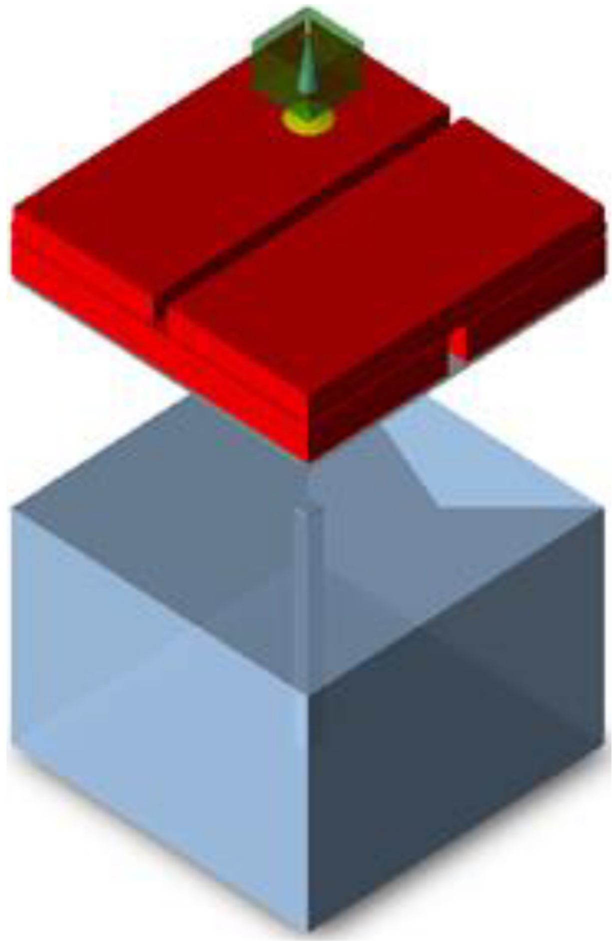

Figure 3. LINAC gantry and water phantom model.

kind is more important to track and which radiation kind is ignored in the cell concerned. Another technique is energy cutoff, which is the removal of photons and particles from the system when they fall below a certain energy level as a result of interactions.

The model created in the MCNP code language was visualized using the Vised (visual editor) software included in the MCNP installation package [13]. Figure 4 shows the photon tracking image for increasing numbers of electrons. The photons are represented by the color scale according to the energy they interact with.

3. Results and discussion

Electrons generated in the source cell were accelerated to the target by moving in the vacuum tube and X-rays were produced. The X-rays were shaped in the primary and secondary collimators, flattened in flattening filters, and measured in the water phantom through the ion chamber.

The PDD and dose profile values obtained by simulations with different fields were compared with experimental data obtained with the linear accelerator in a clinic for filtered and FFF systems and the results were found to be consistent. The PDD values obtained for the filtered system also overlap with the British Journal of Radiology (BJR) values [14]. For each energy value, by controlling the specific factors such as depth

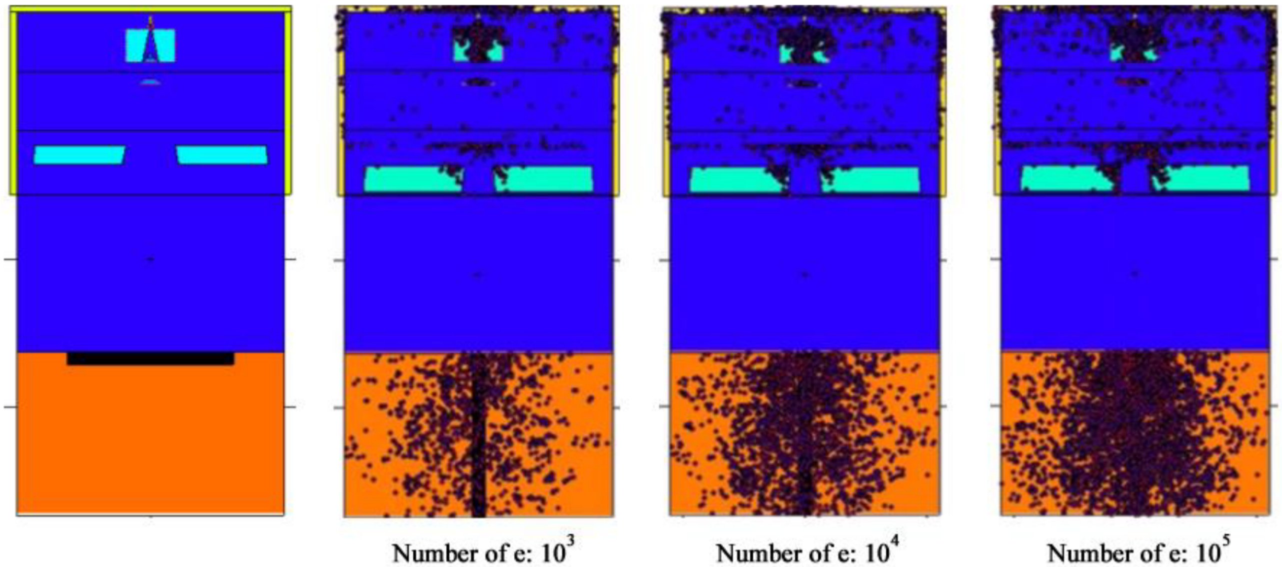

Figure 4. Simulation view with VISED code.

at which the maximum dose occurs and the ratio of dose measured at 20 cm depth and dose measured at 10 cm depth (D20/D10), the device ensures photon production in the correct energy. When the PDD values obtained in the filtered system for the 10 $\times$ 10 cm^2 irradiation area shown in Figure 5 were examined, the dose maximum point was determined at 3.25–3.50 cm in depth. The theoretical value of the maximum depth of the dose is 3.2 cm [9].

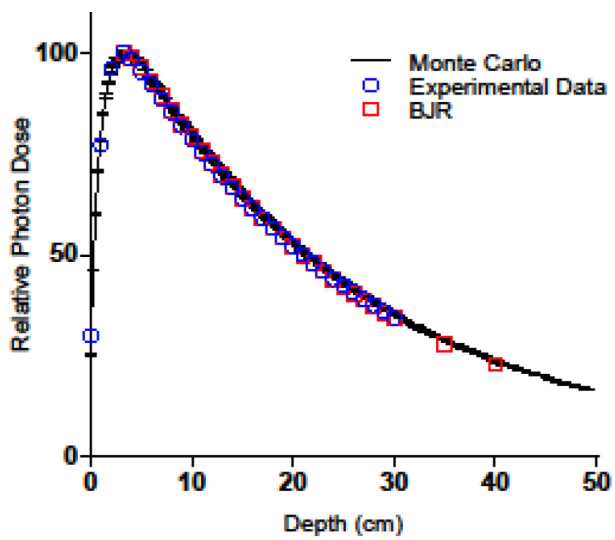

Figure 5. Comparison of Monte Carlo values with experimental and theoretical PDD values at 18 MV, 10 $\times$ 10 cm^2, filtered.

One of the main parameters in photon energy control is the D20/D10 value. It shows a change depending on the dose with depth. In the Table, simulation values, theoretical values, and experimental values are shown and compared. When simulations performed for all areas were evaluated, the maximum errors in the comparison of simulation–experimental and simulation–BJR values were found to be 0.22% and 1.24%, respectively.

Table. Comparison of Monte Carlo D20/D10 values with experimental and theoretical values at 18 MV, filtered.

Field (cm^2)	Monte Carlo	Experimental	BJR	MC-experimental error %	MC-BJR Error %
10 × 10	0.6665 ±0.0034	0.6650 ±0.0004	0.65	+0.22 ±0.0034	−1.24 ±0.0034
20 × 20	0.6810 ±0.0035	0.6823 ±0.0003	0.67	–0.19 ±0.0035	+0.50 ± 0.0035
40 × 40	0.6982 ±0.0034	0.6976 ±0.0004	0.69	+0.08 ±0.0034	+0.85 ±0.0034

Figures 6 and 7 show dose profiles for all irradiation fields of the simulated and experimental results in the filtered and FFF systems. The results were found to match each other.

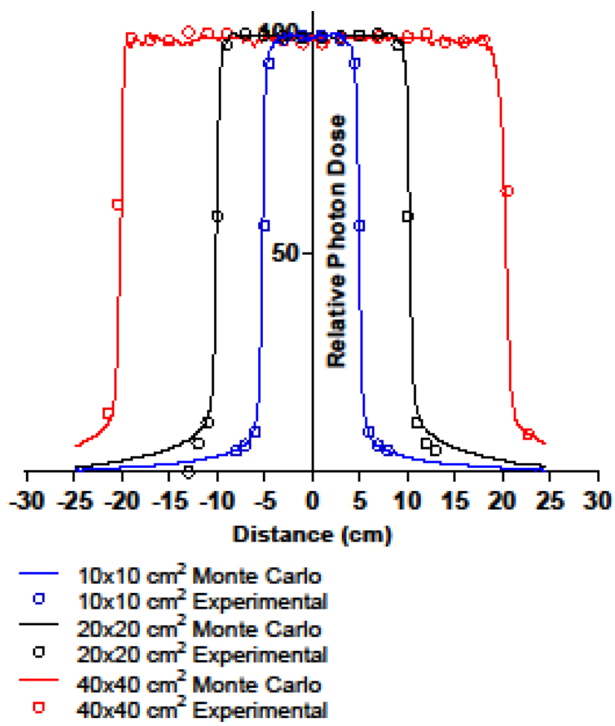

Figure 6. Comparison of Monte Carlo values with experimental dose profile values at 18 MV, filtered.

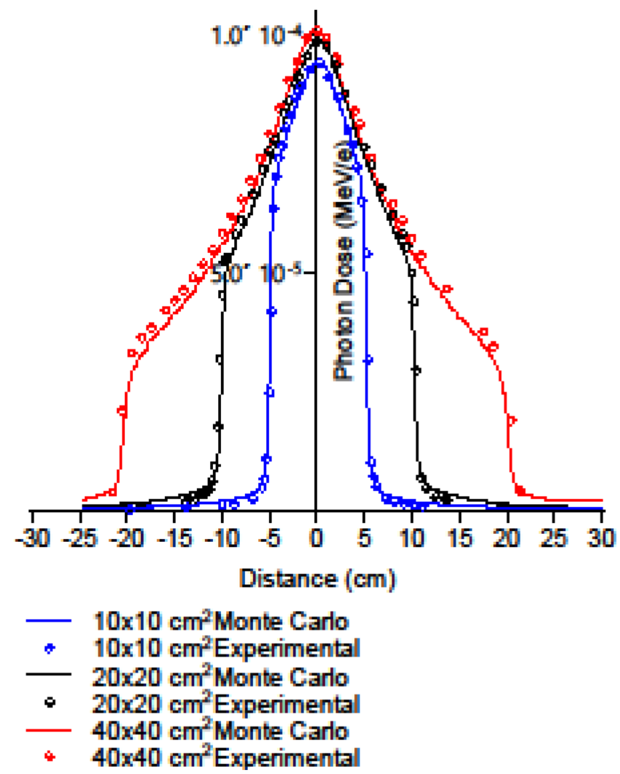

Figure 7. Comparison of Monte Carlo values with experimental dose profile values at 18 MV, FFF.

When the photon spectrum obtained from 100 cm of SSD in the air environment for the filtered system is examined, it is determined that the maximum photon flux is seen at the channel representing the energy range of 0.51–0.52 MeV, which is annihilation photon energy (0.511 keV). When interacting photon energy is at 1.02 MeV or higher, pair production may occur and the photon is split into an electron–positron pair. As the positron comes to a rest, it combines with an electron. Two annihilation photons, each of 0.511 MeV in energy, travel at 180° to each other. As the energy increases, more photons in the spectrum will be higher than the pair production energy and, as a result, at 18 MV, according to 6 MV, more annihilation photons will be produced. Except for annihilation photons, the highest photon density is at 1.42 MeV and the mean energy is 4.82 MeV. When the photon spectrum obtained in the FFF system is examined, the peak is again in the range of 0.51–0.52 MeV. The maximum photon flux, excluding the peak, is detected at 0.48 MeV. The average photon energy is 3.54 MeV.

The photon spectra obtained at SSD of 100 cm, 110 cm, 120 cm, and 130 cm in filtered and FFF systems with 10 × 10 cm^2 irradiation field are shown in Figures 8 and 9. When the spectra were examined, it was determined that the distribution of photon flux decreased with increasing distance. The average photon energy is 4.82 MeV, 4.84 MeV, 4.86 MeV, and 4.87 MeV in the filtered system and 3.54 MeV, 3.55 MeV, 3.55 MeV, and 3.56 MeV in the FFF system at distances of 100 cm, 110 cm, 120 cm, and 130 cm, respectively.

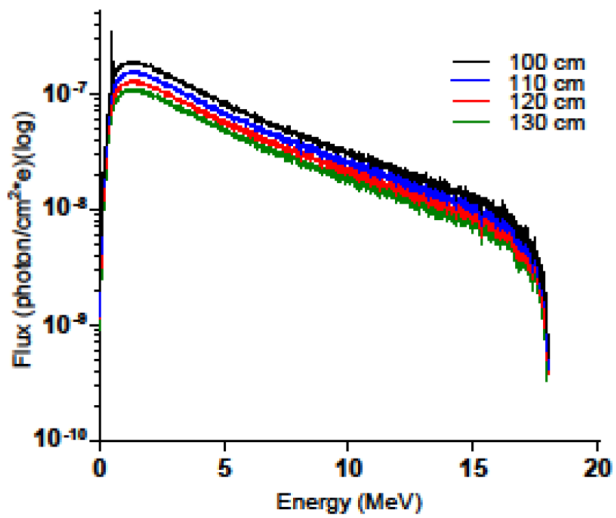

Figure 8. Photon spectrum at different distances from the target at 18 MV, 10 × 10 cm^2, filtered.

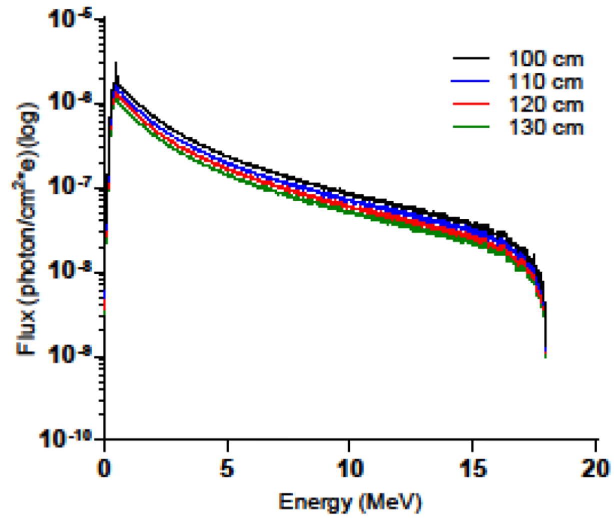

Figure 9. Photon spectrum at different distances from the target at 18 MV, 10 × 10 cm^2, FFF.

As the low-energy photons are absorbed in the flattening filter, average photon energy is found higher in the filtered system than the FFF system. As shown in Figure 10, it is found that the photon flux obtained from the unit electron in the FFF system is 3.54 times higher than in the filtered system.

Accordingly, the photon dose obtained from the unit electron differs between the filtered and FFF systems, and this difference is shown in Figures 11 and 12. When the PDD curves were examined, the average photon

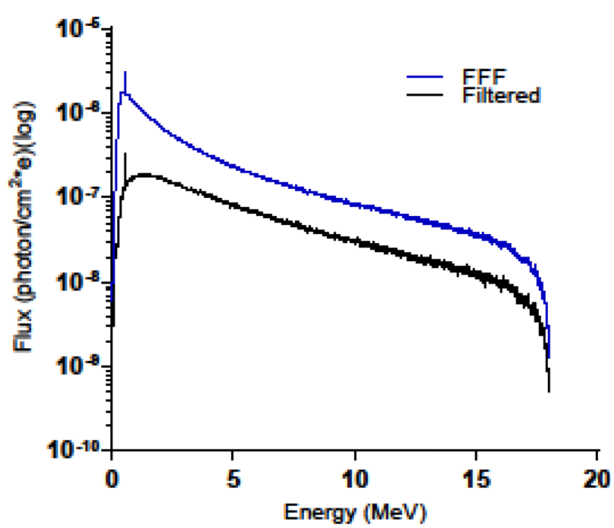

Figure 10. Photon spectra obtained with filtered and FFF systems at a distance of 100 cm from the target at 18 MV, 10 × 10 cm^2.

dose along the depth of the FFF system was found 3.18 times higher than that of the filtered system.

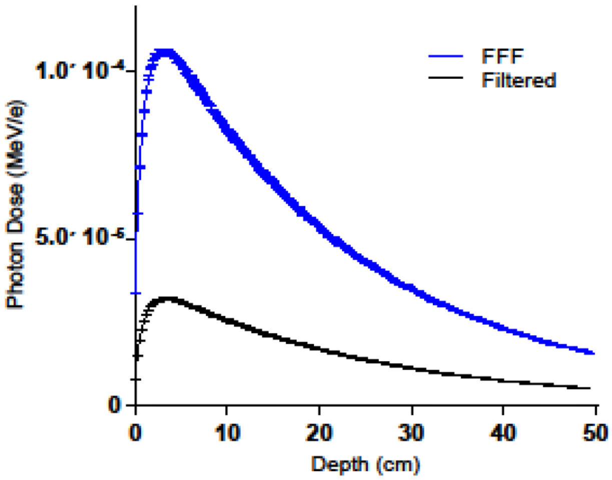

Figure 11. PDD obtained with filtered and FFF systems at a distance of 100 cm from the target at 18 MV, 10 × 10 cm^2.

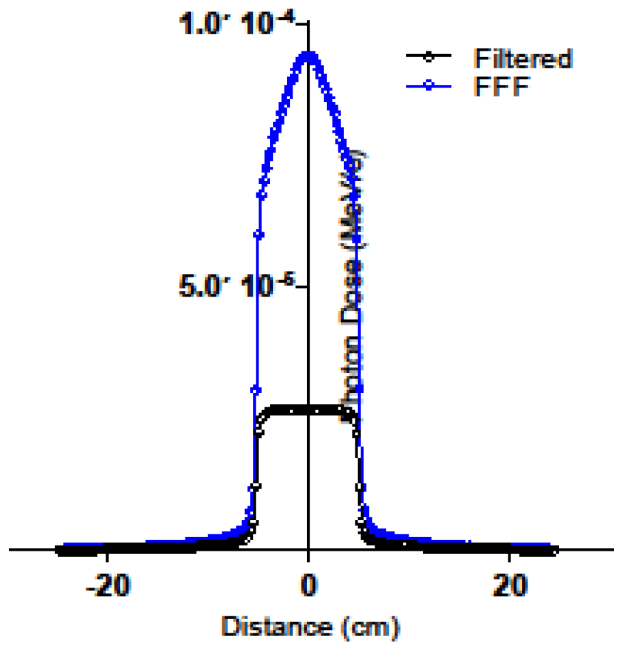

Figure 12. Dose profile obtained with filtered and FFF systems at a distance of 100 cm from the target at 18 MV, 10 × 10 cm^2.

4. Conclusion

In this study, a medical electron linear accelerator was modeled with all the components of the gantry and a detailed simulation was performed with the MC method. The data obtained by using the MCNP code provided a detailed analysis of the working principles for the filtered and FFF systems of the linear accelerator. The developed model can be used in further studies.

References

[1] Halperin, E. C.; Perez, C. A.; Brady, L. W. *Principles and Practice of Radiation Oncology*, 5th ed.; Lippincott Williams & Wilkins: Philadelphia, PA, USA, 2008.

[2] Kim, S. J. *J. Korean Phys. Soc.* **2015**, *67*, 153-158.

[3] Goorley, J. T.; James, M. R.; Booth, T. E.; Brown, F. B.; Bull, J. S.; Cox, L. J.; Durkee, J. W.; Elson, J. S.; Fensin, M. L; Forster, R. A. et al. *MCNP6.1.1-Beta Release Notes (LA-UR-14-24680)*; Los Alamos National Laboratory: Los Alamos, NM, USA, 2014.

[4] Wu, Y.; Song, J; Zheng, H.; Sun, G.; Hao, L.; Long, P.; Hu, L. *Ann. Nucl. Energy* **2015**, *82*, 161-168.

[5] Kaur, G.; Pickrell, G. R. *Modern Physics*, 1st ed.; McGraw-Hill Education: New Delhi, India, 2014.

[6] Kretschmer, M.; Sabatino, M.; Blechschmidt, A.; Heyden, S.; Grünberg, B.; Würschmidt, F. *Radiat. Oncol.* **2013**, *8*, 133.

[7] Lee, M.; Lim, H.; Lee, M.; Yi, J.; Rhee, D. J.; Kang, S. K.; Jeong, D. H. *Prog. Med. Phys.* **2015**, *26*, 99-105.

[8] Buzdar, S. A.; Rao, M. A.; Nazir, A. *Journal of Ayub Medical College* **2009**, *21*, 41-5.

[9] Mayles, P.; Nahum, A.; Rosenwald, J. C. *Handbook of Radiotherapy Physics, Theory and Practice*, 1st ed.; Taylor & Francis Group: London, UK, 2007.

[10] Constantin, M.; Perl, J.; Losasso, T.; Salop, A.; Whittum, D.; Narula, A.; Svatos, M.; Keall, P. J. *Med. Phys.* **2011**, *38*, 4018-4024.

[11] Harris, G. M. MSc, Georgia Institute of Technology, Atlanta, GA, USA, 2012.

[12] Hendricks, J. S.; Booth, T. E. In Alcouffe, R.; Dautray, R.; Forster, A.; Ledanois, G.; Mercier, B., Eds. *Monte-Carlo Methods and Applications in Neutronics, Photonics and Statistical Physics*; Springer: Berlin, Germany, 1985.

[13] Schwarz, R.; Carter, L. L.; Schwarz, A. *Modification to the Monte Carlo N-Particle (MCNP) Visual Editor (MCNPVised) to Read in Computer Aided Design (CAD) Files (Final Report)*; Office of Science and Technical Information: Washington, DC, USA, 2005

[14] British Journal of Radiology. *Br. J. Radiol.* **1983**, *17* (Suppl.).